crystals

MDPI

Article

Thermodynamic Properties of $MgAl_2O_4$ Spinel at High Temperatures and High Pressures

Wuxueying Qiu [1], Chang Su [1,2,3,*], Yonggang Liu [2,*] and Wei Song [2]

[1] School of Earth Sciences, Institute of Disaster Prevention, Sanhe 065201, China
[2] Key Laboratory of High Temperature and High Pressure Study of the Earth's Interior, Institute of Geochemistry, Chinese Academy of Sciences, Guiyang 550081, China
[3] Hebei Key Laboratory of Earthquake Dynamics, Sanhe 065201, China
* Correspondence: suchang@cidp.edu.cn (C.S.); liuyonggang@vip.gyig.ac.cn (Y.L.)

Abstract: Thermodynamic properties of $MgAl_2O_4$ spinel are significant in understanding the phase relations of the Earth's crust and upper mantle, but available values from experimental measurements are limited at ambient pressure conditions to date. Based on an iterative numerical approach and experimental data from the literature, we determined the self-consistent unit-cell volume, elastic moduli, and, particularly, thermodynamic properties, including thermal expansion, heat capacity, entropy, and the Grüneisen parameter of $MgAl_2O_4$ spinel over a wide temperature and pressure range. The obtained thermal expansion, heat capacity, entropy, and Grüneisen parameter of $MgAl_2O_4$ spinel show nonlinearly and are negatively correlated with pressure. Most importantly, we found that the pressure effects on thermal expansion and entropy increase with temperature, whereas the pressure effect on the heat capacity and the Grüneisen parameter decreases to a minimum at ~400 K and ~700 K, respectively, then increases or remains almost constant above this temperature, respectively.

Keywords: spinel; thermal expansion; heat capacity; entropy; Grüneisen parameter;high temperatures and high pressures

Citation: Qiu, W.; Su, C.; Liu, Y.; Song, W. Thermodynamic Properties of $MgAl_2O_4$ Spinel at High Temperatures and High Pressures. *Crystals* **2023**, *13*, 240. https://doi.org/10.3390/cryst13020240

Academic Editors: Yuri N. Palyanov and Russell Hemley

Received: 7 December 2022
Revised: 20 January 2023
Accepted: 25 January 2023
Published: 30 January 2023

1. Introduction

Magnesium aluminum spinel ($MgAl_2O_4$) is one of the simple high-density oxides of very abundant chemical elements on Earth, and it is also an important host mineral for aluminum and other trivalent cations in the shallow upper mantle [1]. Moreover, due to its excellent chemical, thermal, dielectric, mechanical, and optical properties, $MgAl_2O_4$ spinel is also an indispensable material in various scientific and industrial applications [2,3].

Petrology and geochemistry evidence suggests that the plagioclase-spinel and spinel-garnet phase transitions are considered to be two key boundaries at the top upper mantle, which are significant for investigating the processes of heterogeneity in the upper mantle rocks [4]. Therefore, the equation of state (EoS) of $MgAl_2O_4$ spinel has been widely carried out using various experimental methods [5–16], which provide abundant data to derive the composition and density structure of the upper mantle. In contrast, the experimental data on the thermodynamic properties, such as thermal expansion, heat capacity, entropy, and the Grüneisen parameter, of $MgAl_2O_4$ spinel at simultaneous high temperature and high pressure conditions (HT-HPs) are still scarce.

To provide a better understanding of the thermodynamic properties, as well as the subsolidus phase relations and phase transformations, of the upper mantle, a comprehensive set of thermodynamic data for all involved mineral phases is needed. However, most of the previous investigations on the thermodynamic properties of $MgAl_2O_4$ spinel were performed at ambient pressure conditions. For example, the thermal expansion of $MgAl_2O_4$ spinel at ambient pressure conditions was determined through dilatometric measurements directly [17,18], or can be derived from its specific volume as a function of temperature

obtained via experimental measurements, such as X-ray diffraction [19–23] and neutron diffraction [24–26]. However, empirical EoS, such as the third-order Birch-Murnaghan (3BM) EoS [27] or the Mie–Grüneisen–Debye (MGD) EoS [28], are required to derive the thermal expansion at HT-HPs, in which empirical parameters were used during the calculations. For example, the pressure derivative of the isothermal bulk modulus is assumed to be a constant in 3BM EoS, and the Grüneisen parameter is a function of volume only in MGD EoS. In the meantime, because of the limitation of the calorimetric measurements, the experimentally determined heat capacities [29–32] and entropies [29,32] of $MgAl_2O_4$ spinel were also constrained at ambient conditions.

With the development of a computer simulation, the first principle calculations [33] and theoretical calculations based on the published EoS [16,34,35] definitely provide us with efficient ways to estimate the thermodynamic properties of minerals and phase transition boundaries at HT-HPs. However, the separations between the results from these theoretical works are nonnegligible, and there are still considerable controversies about the thermodynamic properties of $MgAl_2O_4$ spinel at HT-HPs, especially the pressure effects on these thermodynamic properties. Earlier, Davis and Gordon [36] introduced an iterative numerical approach, following which the self-consistent density, thermal expansion, and heat capacity, particularly, of melts at HT-HPs could be derived from the density and heat capacity at ambient pressure conditions, as well as the adiabatic elastic wave velocity at HT-HPs. The advantage of this method is that all the obtained values are determined completely based on the experimental data, without using any empirical parameters. The feasibility of this method later has been proved on melts [37,38] and minerals [39–41]. Thus, the thermodynamic properties at HT-HPs can be determined totally based on the experimental data of minerals conveniently.

In this study, we aim to constrain the values of thermodynamic properties of $MgAl_2O_4$ spinel at HT-HPs using the iterative numerical approach. Based on the experimental data from the literature, we derived the self-consistent unit-cell volume, adiabatic bulk modulus, shear modulus, and the thermodynamic properties, including thermal expansion, heat capacity, entropy, and the Grüneisen parameter of $MgAl_2O_4$ spinel in a wide temperature and pressure range. Then, comparisons were made with available published data to confirm the accuracy of our obtained results. Additionally, the pressure effects on these thermodynamic properties were reported.

2. Methods

2.1. Calculation Procedure

The method used in this study is summarized in our recent studies [39–41], and the fundamental procedure is described below. The uncertainties of the derived parameters at different temperature (T) and pressure (P) conditions are estimated using the Taylor series expansion based on the experimental measuring error, as well as the uncertainties of the fitting coefficients.

The thermal expansion (α) at constant pressure is related to volume (V) as Equation (1), and the integration of Equation (1) yields Equation (2), where V_0 represents the volume at ambient conditions.

$$\alpha(T) = \frac{1}{V}\left(\frac{\partial V}{\partial T}\right) \tag{1}$$

$$V(T) = V_0 exp\left[\int_{T_0}^{T} \alpha(T)dT\right] \tag{2}$$

Then, the isothermal derivative of volume with respect to pressure can be written as Equation (3), where C_P stands for heat capacity, v_Φ refers to the bulk sound velocity. The bulk sound velocity is related to the specific volume and adiabatic bulk modulus (K_S) by $v_\Phi = (VK_S)^{1/2}$, which can be calculated from the P-wave velocity (v_P) and S-wave velocity

(v_S) by Equation (4). Meanwhile, the isothermal derivative of the heat capacity with respect to pressure can be evaluated by Equation (5).

$$\left(\frac{\partial V}{\partial P}\right)_T = -V^2\left(\frac{1}{v_\Phi^2} + \frac{T\alpha^2}{C_P}\right) \tag{3}$$

$$v_\Phi = \left(v_p^2 - \frac{4}{3}v_s^2\right)^{\frac{1}{2}} \tag{4}$$

$$\left(\frac{\partial C_P}{\partial P}\right)_T = -VT\left[\alpha^2 + \left(\frac{\partial \alpha}{\partial T}\right)_P\right] \tag{5}$$

To start the calculation, firstly, we use the experimentally determined volume at ambient pressure conditions to obtain the thermal expansion as a function of temperature via Equation (1). In the meantime, we need to fit the v_P and v_S with a suitable formula to get the pressure and temperature dependences of the bulk velocity via Equation (4). With the obtained thermal expansion and heat capacity as a function of temperature at ambient pressure, the approximate volume at an arbitrary reference pressure could be estimated using Equation (3). The resulting volume at this reference pressure can be used to update the value of thermal expansion and heat capacity at the same pressure with Equation (1) and Equation (5), respectively. Hence, the iteration of this loop leads to converged volume, thermal expansion, and heat capacity as a function of temperature and pressure based on the experimental elastic wave velocity at HT-HPs.

With the determined volume, as well as v_P and v_S at HT-HPs. The adiabatic bulk modulus and shear modulus (G) can be obtained using Equation (6) and Equation (7), respectively.

$$K_S = \frac{1}{V}\left(v_p^2 - \frac{4}{3}v_s^2\right) \tag{6}$$

$$G = \frac{1}{V}v_S^2 \tag{7}$$

Additionally, since the temperature and pressure dependences of entropy (S) are related to the heat capacity and thermal expansion via Equation (8) and Equation (9), respectively, with the standard entropy measured at ambient conditions, the entropy at HT-HPs can also be derived [42]. Furthermore, the Grüneisen parameter can be deduced from the obtained parameters above using Equation (10).

$$S(T)_P = S(T_0)_P + \int_{T_0}^{T}\left(\frac{C_P}{T}\right)dT \tag{8}$$

$$S(P)_T = S(P_0)_T - \int_{P_0}^{P}\alpha V dP \tag{9}$$

$$\gamma = \frac{\alpha K_S V}{C_P} \tag{10}$$

2.2. Thermoelastic Data of $MgAl_2O_4$ Spinel

2.2.1. Elastic Wave Velocity at High-Temperature and High-Pressure Conditions

The elastic wave velocity of $MgAl_2O_4$ spinel was determined at ambient pressure conditions by Askarpour et al. [8] using Brillouin scattering to 1273 K, and the result showed that both v_P and v_S were linearly correlated with the temperature. Later, Suzuki et al. [11] reported the elastic properties of $MgAl_2O_4$ spinel using the resonant sphere technique, from which the elastic wave velocity could be also derived in the temperature range of 293–1167 K. Then, Zou et al. [14] measured the elastic wave velocity of $MgAl_2O_4$ spinel at simultaneously high temperature and high pressure conditions using ultrasonic interferometry, in which they suggested the linear temperature and pressure dependences of both

v_P and v_S. Very recently, Duan et al. [15] also presented the elastic velocity of $MgAl_2O_4$ spinel using Brillouin scattering up to 10.9 GPa and 1000 K in diamond anvil cells. It is worth noting that although the order to disorder transition in $MgAl_2O_4$ spinel would cause a small change in the temperature dependence of shear modulus at ~923 K [8,11], its effects on v_P and v_S are rather weak and thus can be ignored [14,15]. Therefore, we fit the P- and S-wave velocities data summarized in Table 1 [8,11,14,15] with Equation (11). The fitting coefficients and their uncertainties are listed in Table 2, where the pressure is expressed in GPa, the temperature is expressed in K, and the P- and S-wave velocities are expressed in m/s. Note that although the fitting quality of Equation (11) is relatively great at HT-HPs, Equation (11) is not suitable for estimating the elastic wave velocity $MgAl_2O_4$ spinel in the temperature range below room temperature.

$$v(P,T) = v_0 + v_1 P + v_2 (T - 273) \quad (11)$$

Table 1. Elastic velocity, unit-cell volume, heat capacity, and entropy data of $MgAl_2O_4$ spinel used in this study.

Data Type	Temperature Range	Pressure Range	Method	References
	K	GPa		
Elastic wave velocity	300–1273	Ambient	Brillouin scattering	Askarpour et al. (1993) [8]
	293–1167	Ambient	Resonant sphere technique	Suzuki et al. (2000) [1] [11]
	300–900	5.3–14.2	Ultrasonic interferometry	Zou et al. (2013) [14]
	300–1000	0–10.9	Brillouin scattering	Duan et al. (2018) [2] [15]
Unit-cell volume	299–1073	Ambient	X-ray diffraction	Singh et al. (1975) [3] [19]
	293–1933	Ambient	X-ray diffraction	Yamanaka and Takeuchi (1983) [20]
	293–1273	Ambient	Neutron diffraction	Peterson et al. (1991) [24]
	77–300	Ambient	X-ray diffraction	Grimes and Al-Ajaj (1992) [21]
	299–1662	Ambient	Neutron diffraction	Redfern et al. (1999) [25]
	298–1927	Ambient	X-ray diffraction	Fiquet et al. (1999) [22]
	300–1700	Ambient	Neutron diffraction	Pavese et al. (2000) [26]
	298–1223	Ambient	X-ray diffraction	Carbonin et al. (2002) [4] [23]
Heat capacity	53.55–298.16	Ambient	Calorimeter	King (1955) [29]
	421.0–1805.5	Ambient	Calorimeter	Bonnickson (1955) [30]
	862.8–1806.9	Ambient	Calorimeter	Richet and Fiquet (1991) [22]
	4.33–305.2	Ambient	Calorimeter	Klemme and Ahrens (2007) [32]
Standard entropy	298.15	Ambient	Calorimeter	Klemme and Ahrens (2007) [32]

[1] Elastic wave velocity derived from the elastic moduli and density [11]. [2] Elastic wave velocity derived from the elastic moduli and density [15]. [3] Unit-cell volume data calculated from the observed lattice parameter of synthetic spinel [19]. [4] Unit-cell volume data calculated from the lattice parameter of synthetic $Mg_2Al_2O_4$ spinel during heating [23].

Table 2. Fitting coefficients and their uncertainties of Equation (11) to calculate the P- and S-wave velocities of $MgAl_2O_4$ spinel at HT-HPs.

Elastic Wave Velocity	v_0	v_1	v_2
v_P	9825 (10)	40.1 (9)	−0.354 (14)
v_S	5514 (9)	−1.8 (8)	−0.215 (13)

2.2.2. Thermal Expansion at High-Temperature and Ambient Pressure Conditions

Lattice parameters of $MgAl_2O_4$ spinel at ambient pressure conditions have been measured using X-ray diffraction [19,20,22,23] and neutron diffraction [24–26] from room temperature to ~1900 K, and the values at the low-temperature range were provided by Grimes and Al-Ajaj [21] (Table 1, Figure 1). Although previous investigations reported that the order-disorder transition would affect the volume as well as the thermal expansion of $MgAl_2O_4$ spinel [11,17,20,43–45], due to the limitations of the method used in this study, we assume that the ordering state of the cations does not affect the volume. Therefore, we converted the lattice parameters of $MgAl_2O_4$ spinel from the published literature [19–26] (Table 1) to the unit-cell volumes, then analyzed the values via the EoSfit software [46] and

fit them using the empirical formula recommended by Fei [47]. The obtained equation for the thermal expansion of $MgAl_2O_4$ spinel as a function of temperature is shown as Equation (12). The unit-cell volume of $MgAl_2O_4$ spinel calculated via Equations (2) and (12) is greatly consistent with the experimental results, and the largest difference is less than 0.5% (Figure 1).

$$\alpha(T) = 2.21(8) \times 10^{-5} + 0.48(8) \times 10^{-8}T - 0.06(8) \times T^{-2} \quad (12)$$

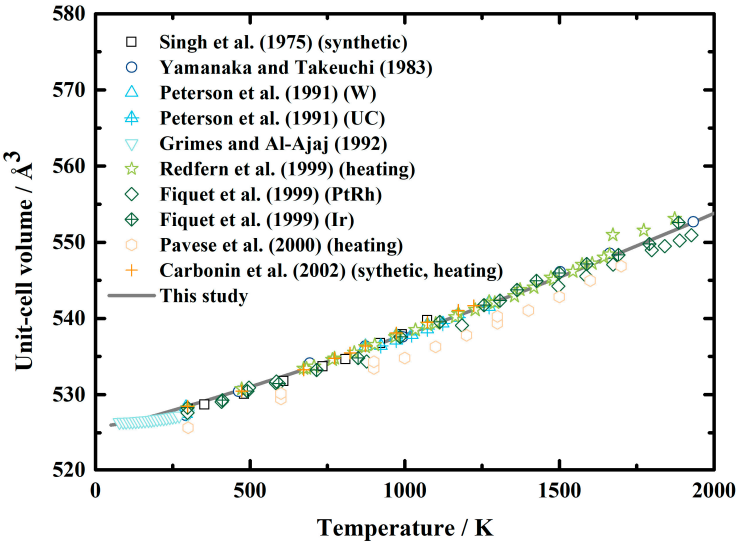

Figure 1. Unit-cell volume of $MgAl_2O_4$ spinel as a function of temperature at ambient pressure conditions. Solid lines: result calculated using Equations (2) and (12) in this study; squares: X-ray diffraction results of Singh et al. [19]; circles: X-ray diffraction results of Yamanaka and Takeuchi [20]; triangles and filled triangles: neutron diffraction results of Peterson et al. [24]; inverted triangles: X-ray diffraction results of Grim and Al-Ajaj [21]; stars: neutron diffraction results collected during heating by Redfern et al. [25]; diamonds and filled diamonds: X-ray diffraction results of Fiquet et al. [22]; hexagons: neutron diffraction results of Pavese et al. [26]; plus signs: X-ray diffraction results of Carbonin et al. [23].

2.2.3. Heat Capacity at High Temperature and Ambient Pressure Condition

The heat capacity of $MgAl_2O_4$ spinel was first determined by King [29] at the temperature range of 53.44~298.15 K. Then the measured temperature was extended to ~1800 K by Bonnickson [30], as well as Richet and Fiquet [31]. Later, the low-temperature heat capacity of $MgAl_2O_4$ spinel was reevaluated by Klemme and Ahrens [32]. Here, we fit these experimentally obtained values using Equations (13)–(15), which are three types of commonly-used empirical formulas recommended by Hass and Fisher [48], Berman and Brown [49], and Richet and Fiquet [31], respectively. The fitting coefficients, as well as the reduced χ^2 and R^2, are listed in Table 3. After comparing the reduced χ^2 and R^2, we decided to use the equation recommended by Richet and Fiquet [31] in this study (Equation (15)). Figure 2 shows the comparisons between the calculated heat capacity of $MgAl_2O_4$ spinel using Equations (13)–(15) and the experimental results from the literature [29–32]. The value was calculated using Equation (15). The largest differences between the values calculated using Equation (15) and the results of King [29], Bonnickson [30], Richet and Fiquet [31], and Klemme and Ahrens [32] are 2%, 2%, 1%, and 5%, respectively, in the temperature range of 200–1800 K. Moreover, the standard entropy used in this study was from Klemme and Ahrens [32] (Table 3), which was determined as S°_{298} = 80.9 (6) J/mol·K.

$$C_P = k_0 + k_1T + k_2T^{-2} + k_3T^{-0.5} + k_4T^2 \quad (13)$$

$$C_P = k_0 + k_1 T^{-0.5} + k_2 T^{-2} + k_3 T^{-3} \quad (14)$$

$$C_P = k_0 + k_1 ln(T) + k_2 T^{-1} + k_3 T^{-2} + k_4 T^{-3} \quad (15)$$

Table 3. Fitting coefficients for the heat capacity of $MgAl_2O_4$ spinel using various empirical formulas.

Fitting Equations	Reduced χ^2	R^2	References of the Empirical Formulas
$C_P = k_0 + k_1 T + k_2 T^{-2} + k_3 T^{-0.5} + k_4 T^2$ $k_0 = 269\ (6)$ $k_1 = 0.015(8)$ $k_2 = 3.02(8) \times 10^5$ $k_3 = -2.80(6) \times 10^3$ $k_4 = -1.3(4) \times 10^{-5}$	18.85	0.991	Hass and Fisher (1976) [48]
$C_P = k_0 + k_1 T^{-0.5} + k_2 T^{-2} + k_3 T^{-3}$ $k_0 = 274(2)$ $k_1 = -2.89(3) \times 10^3$ $k_2 = 4.2(3) \times 10^5$ $k_3 = -4.5(10) \times 10^6$	19.93	0.991	Berman and Brown (1985) [49]
$C_P = k_0 + k_1 ln(T) + k_2 T^{-1} + k_3 T^{-2} + k_4 T^{-3}$ $k_0 = 242(9)$ $k_1 = -8(3)$ $k_2 = -3.87(8) \times 10^4$ $k_3 = 2.2(6) \times 10^6$ $k_4 = -4.26(13) \times 10^7$	5.88	0.997	Richet and Fiquet (1991) [22]

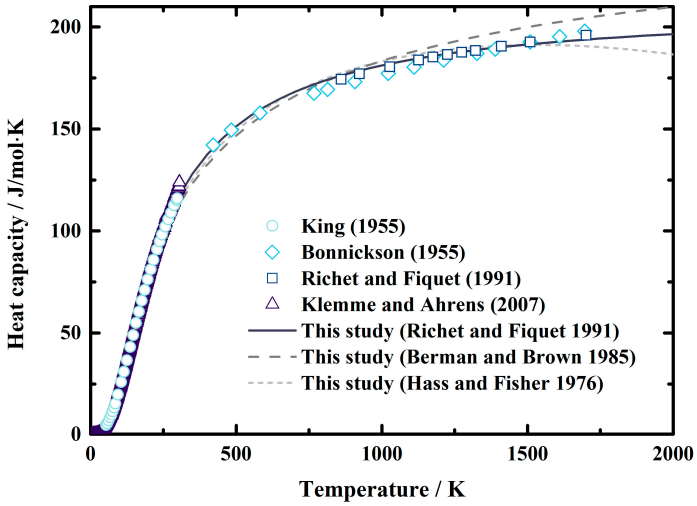

Figure 2. Heat capacity of $MgAl_2O_4$ spinel as a function of temperature at ambient pressure conditions. Short dash line: result calculated using Equation (13) recommended by Hass and Fisher (1976) [48]; dash lines: result calculated using Equation (14) recommended by Berman and Brown (1985) [49]; solid lines: result calculated using Equation (15) Richet and Fiquet (1991) [31]; circles, diamonds, squares, and triangles: results measured using calorimeter by King [29], Bonnickson [30], Richet and Fiquet [31], and Klemme and Ahrens [32], respectively.

3. Results and Discussions

3.1. Elastic Properties at High Temperature and High Pressure Conditions

Figure 3 shows our calculated unit-cell volume of $MgAl_2O_4$ spinel as a function of pressure at various temperatures, along with the results obtained through X-ray diffraction measurements [12,13,15] and theoretical calculations [16] for comparisons. At room temperature conditions, the unit-cell volume from the current study is in good agreement with the data provided by Levy et al. [12] within 0.3%. Meanwhile, excellent consistencies are found when compared with the values published by Nestola et al. [13] and Hagiwara et al. [16],

with the largest differences being less than 0.2% and 0.1%, respectively. Furthermore, the great agreement also holds at high temperature conditions within 0.1% compared to the experimental results of Duan et al. [15].

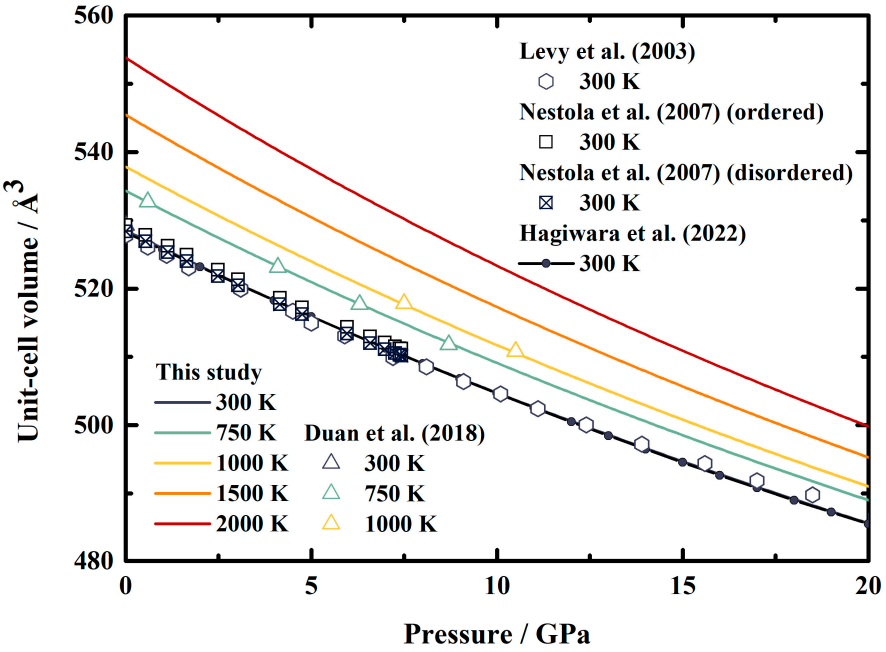

Figure 3. Pressure dependence of the unit-cell volumes of $MgAl_2O_4$ spinel at various temperatures. Solid lines: this study; triangles: X-ray diffraction results of Duan et al. [15]; hexagons: X-ray diffraction results of Levy et al. [12]; squares and filled squares: X-ray diffraction results of ordered and disordered phases, respectively, of Nestola et al. [13]; line and filled circles: theoretical result calculated from the published EoS of $MgAl_2O_4$ spinel by Hagiwara et al. [16].

Based on Equations (6) and (7), we also derived the elastic moduli of $MgAl_2O_4$ spinel at HT-HPs. Both K_S and G generally display linear dependences on temperature and pressure within the uncertainties (Table 4 and Figure 4). The K_S and G at ambient conditions are determined as K_{S0} = 199.8 (13) GPa and G_0 = 108.5 (4) GPa. Additionally, the pressure and temperature derivatives of K_S and G are yielded as $\partial K_S/\partial P$ = 4.126 (12), $\partial G/\partial P$ = 0.420 (5), $\partial K_S/\partial T$ = −0.01787 (8) GPa/K, and $\partial G/\partial T$ = −0.01076 (6) GPa/K.

Table 4. Elastic moduli of $MgAl_2O_4$ spinel at ambient conditions, and their derivatives with respect to pressure and temperature.

K_{S0} GPa	$(\partial K_S/\partial P)_T$	$(\partial K_S/\partial T)_P$ GPa/K	G_0 GPa	$(\partial G/\partial P)_T$	$(\partial G/\partial T)_P$ GPa/K	References
197.4	4.9 (2)	−0.0154 (3)	108.5	0.51 (6)	−0.0094 (1)	Chang and Barsch (1973) [5]
197.9 (2)	5.66 (21)		109	0.4 (5)		Yoneda (1990) [6]
200		−0.019 (1)	109		−0.012 (1)	Askarpour et al. (1993) [8]
210.1		−0.0268 (3)	108.3		−0.0121 (1)	Cynn et al. (1993) [7]
198.2 (8)	5.05 (9)		108.6 (5)	0.072 (7)		Choplas (1996) [9]
197.39 (1)			107.81			Suzuki et al. (2000) [11]
196.0 (9)	4.60 (9)	−0.022 (3)	109.0 (4)	0.58 (3)	−0.014 (1)	Zou et al. (2013) [14]
197 (1)	4.5 (2)		98.3 (4)	0.36 (6)		Speziale et al. (2016) [50]
198 (1)	4.0 (2)	−0.017 (2)	107 (1)	0.18 (2)	−0.008 (3)	Duan et al. (2018) [15]
198 (2)			108 (1)			Bruschini et al. (2018) [51]
200 (1)			106.7 (5)			Núñez-Valdez et al. (2018) [1] [52]
199.8 (13)	4.126 (12)	−0.01787 (8)	108.5 (4)	0.420 (5)	−0.01076 (6)	This study

[1] Determined using Brillion scattering, the value of G_0 is calculated from $G = (G_{voigt} + G_{Reuss})/2$.

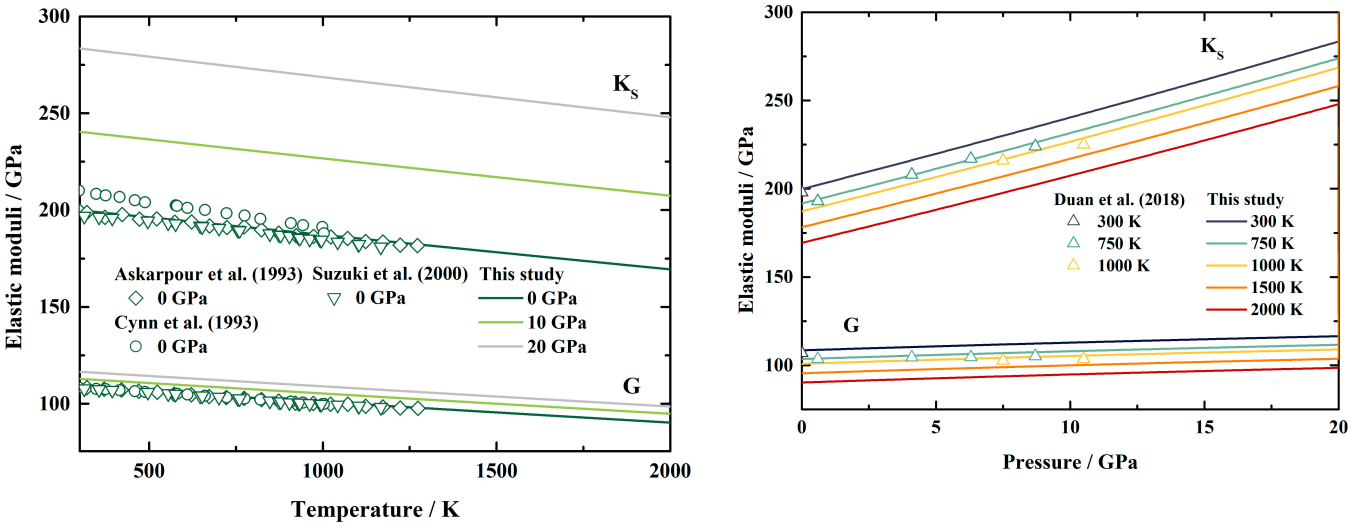

Figure 4. The adiabatic bulk modulus and shear modulus of $MgAl_2O_4$ spinel as a function of temperature (**a**) and pressure (**b**). Solid lines: this study; diamonds: Brillouin scattering measurements by Askarpour et al. [8]; circles: Raman and ultrasonic resonance spectra measurements by Cynn et al. [7]; Inverted triangles: resonant sphere measurements by Suzuki et al. [11]; triangle: Brillouin scattering measurements by Duan et al. [15].

Table 4 lists the available values of the elastic moduli of $MgAl_2O_4$ spinel [5–9,11,14,15,50–52]. Generally, our obtained K_{S0} is close to the results of Askarpour et al. [8] and Bruschini et al. [51], and lower than the results of Cynn et al. [7] and Núñez-Valdez et al. [52]. Additionally, our K_{S0} is slightly higher than the other values listed in Table 4 [5,6,9,11,14,15,50], which is probably caused by the assumption of the linear relationship between the temperature and the elastic wave velocity of $MgAl_2O_4$ spinel (Equation (11)). Our $\partial K_S/\partial P$ is consistent with that of Duan et al. [15], but lower than the other values in Table 4 [5–9,11,14,50–52]. Besides, our $\partial K_S/\partial T$ also shows good agreement with the results of Duan et al. [15], and is generally within the range of the available values [5,6,8,14]. Meanwhile, the values of G_0 determined from previous work vary in a large range from 98.3 GPa to 109 GPa (Table 4). The G_0 in this study is close to most of the results in Table 4 [5–9,14,15,51]. Moreover, our $\partial G/\partial P$ and $\partial G/\partial T$ are within the range of the available values listed in Table 4 [5–8,14,15,50].

Figure 4a,b illustrates the temperature and pressure dependences of our K_S and G, along with previous experimental results for comparisons [7,8,11,15]. At ambient pressure conditions (Figure 4a), our obtained K_S is slightly larger than the values presented by Askarpour et al. [8] and Suzuki et al. [11], with the largest separations of 1.2% and 1.7%, respectively, which are ~3.3% lower than those of Cynn et al. [7]. In the meantime, the differences between our G and the published results are less than 1.5%, 1.1%, and 1.3% compared with those of Askarpour et al. [8], Cynn et al. [7], and Suzuki et al. [11], respectively (Figure 4a). For high temperature and high pressure conditions (Figure 4b), both K_S and G show good agreement with the values presented by Duan et al. [15], with the largest differences being 1.6% and 1.8%, respectively, at 1000 K.

3.2. Thermodynamic Properties at High Temperature and High Pressure Conditions

The calculated α, C_P, S, and γ of $MgAl_2O_4$ spinel to 20 GPa and 2000 K are presented in Figure 5a–d, respectively. The thermal expansion of mantle minerals is considerably important to investigate the thermodynamic properties of the mantle. However, since a volume error of 1% would possibly lead to a 20% difference in the thermal expansion, large discrepancies can be found between the published thermal expan-

sions of $MgAl_2O_4$ spinel [22]. The thermal expansion at ambient conditions is determined as α_0 = 2.3 (2) × 10^{-5} K^{-1} in this study, which is generally larger than the results of Cynn et al. [7] (2.105 × 10^{-5} K^{-1}), Suzuki et al. [11] (1.790 × 10^{-5} K^{-1} at 313 K), and Hagiwara et al. [16] (1.6765 (10) × 10^{-5} K^{-1}), whereas it is lower than those of Mao et al. [33]. Besides, Figure 5a shows the comparisons between our obtained α and the values presented by Cynn et al. [7], Suzuki et al. [11] at high temperature and ambient pressure conditions, as well as Mao et al. [35] and Hagiwara et al. [17] at HT-HPs. At ambient pressure conditions, our α is larger than the results of Cynn et al. [7] and Hagiwara et al. [16] at room temperature, but becomes lower than those of Cynn et al. [7] and Hagiwara et al. [16] at 577 K and ~800 K, respectively. Then the separations between our α and the values presented by Cynn et al. [7] and Hagiwara et al. [16] increase with the temperature to 9.5% at 1003 K and 8.9% at 2000 K, respectively. As we mentioned in Section 2.2.2, we ignored the effect of order-disorder transition on thermal expansion in this study. Therefore, our calculated α does not show a discontinuity with the temperature, which can be observed in the results of Suzuki et al. [11] (Figure 5a). Our obtained value is ~28% higher than the results of Suzuki et al. [11], at 313 K, and ~3% lower than that of Suzuki et al. [11] at 934 K. For high pressure conditions, our result is quite lower than that of Mao et al. [33]. On the other side, though at ambient pressure conditions, the differences between our results and those of Hagiwara et al. [16] are quite large, the separations decrease to ~1.5% above ~850 K at 10 GPa and 20 GPa.

Figure 5b presents the temperature dependence of the calculated C_P at 0 GPa, 10 GPa, and 20 GPa, along with previous results at ambient pressure conditions [53,54] and high-pressure conditions [16,33]. Both Berman [53] and Robie and Hemingway [54] fitted the experimental data by Bonnickson [30] and provided the fitting equations for the C_P of $MgAl_2O_4$ spinel as a function of temperature to 1800 K. Our calculated C_P at 0 GPa generally agree with the results of Berman [53] and Robie and Hemingway [54], and the separations are within 1.6% and 1.8%, respectively. For high-temperature and high-pressure conditions, our result is quite a bit lower than that of Mao et al. [33]. Additionally, the C_P determined in this study, as well as by Berman [53] and Robie and Hemingway [54], are generally larger than that determined by Hagiwara et al. [16]. The reason is probably because the result obtained by Hagiwara et al. [16] was based on the Mie–Grüneisen–Debye EoS, which uses a very simplified phonon density of state.

Currently, the experimentally determined entropy of $MgAl_2O_4$ spinel is limited at ambient pressure conditions [29,32]. With the combination of the standard entropy from calorimetric measurements [32] and our determined C_P at HT-HPs, the S of $MgAl_2O_4$ spinel at HT-HPs can be calculated via Equations (8) and (9). Our result shows a good agreement with the data of Robie and Hemingway [54] within 0.7% (Figure 5c). Additionally, our values are within the results derived using first-principle calculations by Mao et al. [33] and the EoS of $MgAl_2O_4$ spinel by Hagiwara et al. [16].

The Grüneisen parameter is a valuable thermodynamic parameter in geophysics, which can be used to set limitations on the pressure and temperature dependence of the thermal properties of the Earth's interior [55]. Therefore, we also present the Grüneisen parameter of $MgAl_2O_4$ spinel at HT-HPs, and the result is illustrated in Figure 5d. The ambient condition Grüneisen parameter of $MgAl_2O_4$ spinel is determined as γ_0 = 1.57 (13), which is close to the value of Cynn et al. [7] (γ_0 = 1.52), but higher than that of Suzuki et al. [11] (γ_0 = 1.17) and Hagiwara et al. [16] (γ_0 = 1.136 (11)), whereas it is lower than that of Mao et al. [33] (γ_0 = 1.907). Our γ decreases rapidly with the temperature to ~1200 K, then increases slightly with temperature with very small temperature derivations of 0.00003/K, 0.00002/K, and 0.00001/K at 0 GPa, 10 GPa, and 20 GPa, respectively, which shows a similar pattern as that of Mao et al. [33] and Hagiwara et al. [16]. However, our calculated γ is generally lower than the result of Mao et al. [33] and Hagiwara et al. [16]. Additionally, since the Grüneisen parameter is related to the thermal expansion (Equation (10)), our obtained γ does not show the anomaly at ~900 K as the result of Suzuki et al. do [11].

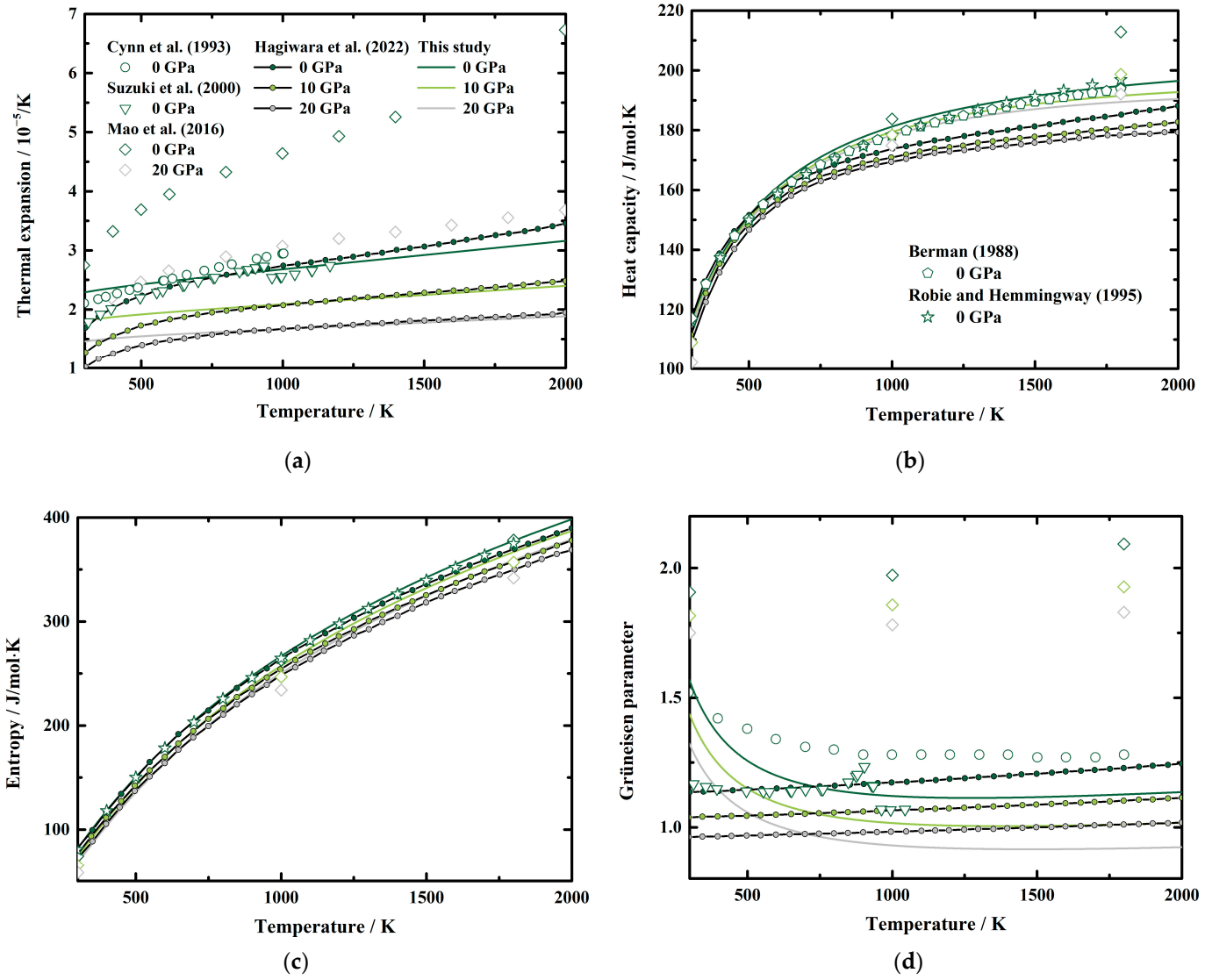

Figure 5. Temperature dependence of the (**a**) thermal expansion, (**b**) heat capacity, (**c**) entropy, and (**d**) Grüneisen parameter of $MgAl_2O_4$ spinel at various pressures. Solid lines: this study; circles and inverted triangles: results of Cynn et al. [7] and Suzuki et al. [11], respectively, at ambient pressure conditions; diamonds: first-principles calculations results of Mao et al. [33]; line and filled circles: theoretical result calculated from the published EoS of $MgAl_2O_4$ spinel by Hagiwara et al. [16]; pentagon and stars: results of Berman [53] and Robie and Hemingway [54] determined from calorimetric measurements by Bonnickson [30].

3.3. Pressure Effects on the Thermodynamic Properties of $MgAl_2O_4$ Spinel

To investigate the pressure effect on the thermodynamic properties of $MgAl_2O_4$ spinel, we illustrated our obtained α, C_P, S, and γ as functions of pressure at various temperatures in Figure 6a–d, respectively, together with the results derived using the EoS of $MgAl_2O_4$ spinel by Hagiwara et al. [16]. Considering Figures 5 and 6, it is obvious that all these parameters tend to be negative and nonlinear with increasing pressure, which show the same behavior as the values of Hagiwara et al. [16]. Additionally, we fitted our calculated results to a polynomial equation of $M = M_0 + (\partial M/\partial P)_T \times P + (\partial^2 M/\partial P^2)_T \times P^2$ at fixed temperatures, where M refers to the thermodynamic properties, M_0 refers to M at ambient pressure conditions; and $(\partial M/\partial P)_T$ and $(\partial^2 M/\partial P^2)_T$ refer to the first and second pressure derivatives of M, respectively. The fitting coefficients for α, C_P, S, and γ of $MgAl_2O_4$ spinel are listed in Tables 5–8, respectively.

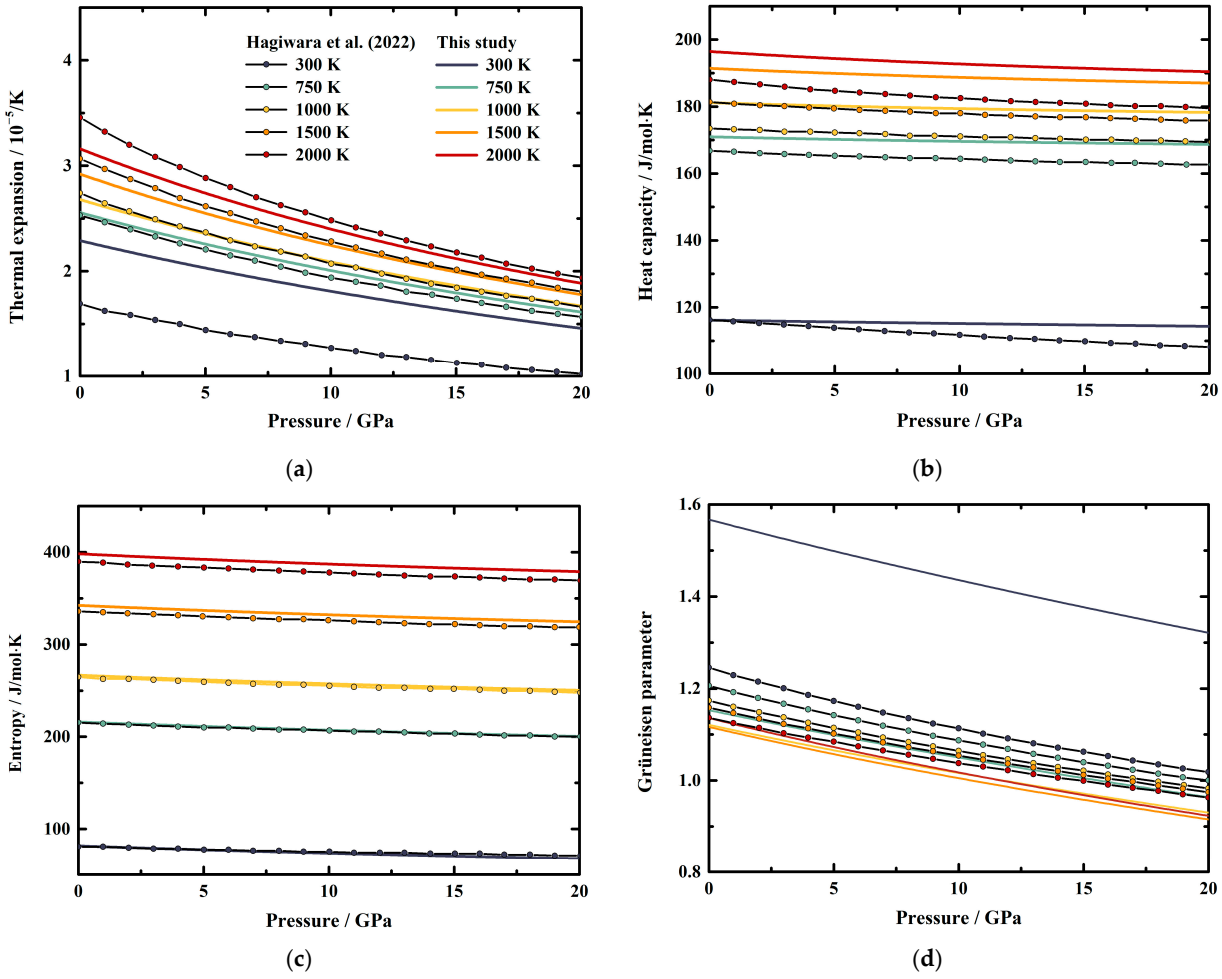

Figure 6. Pressure dependence of the (**a**) thermal expansion, (**b**) heat capacity, (**c**) entropy, and (**d**) Grüneisen parameter of $MgAl_2O_4$ spinel at various pressures. Solid lines: this study; line and filled circles: theoretical result calculated from the published EoS of $MgAl_2O_4$ spinel by Hagiwara et al. [16].

Table 5. The thermal expansion of $MgAl_2O_4$ spinel and their first and second derivatives with respect to pressure at various temperatures.

T K	α_0 10^{-5}/K	$\partial\alpha/\partial P$ 10^{-7}/K·GPa	$\partial^2\alpha/\partial P^2$ 10^{-8}/K·GPa^2
300	2.3 (2)	−5.385 (7)	0.631 (3)
750	2.56 (16)	−6.214 (9)	0.772 (5)
1000	2.68 (17)	−6.713 (11)	0.861 (5)
1500	2.9 (2)	−7.720 (14)	1.040 (7)
2000	3.2 (2)	−8.731 (18)	1.220 (8)

Table 6. The heat capacity of $MgAl_2O_4$ spinel and their first and second derivatives with respect to pressure at various temperatures.

T K	C_{P0} J/mol·K	$\partial C_P/\partial P$ J/mol·K·GPa	$\partial^2 C_P/\partial P^2$ 10^{-3} J/mol·K·GPa^2
300	116 (20)	−0.0921 (3)	–
750	171 (19)	−0.1576 (3)	2.34 (2)
1000	181 (19)	−0.2072 (5)	3.19 (2)
1500	191 (19)	−0.3170 (8)	5.02 (4)
2000	196 (20)	−0.4372 (11)	7.03 (5)

Table 7. The entropy of $MgAl_2O_4$ spinel and their first and second derivatives with respect to pressure at various temperatures.

T K	S_0 10^2 J/mol·K	$\partial S/\partial P$ J/mol·K·GPa	$\partial^2 S/\partial P^2$ 10^{-2} J/mol·K·GPa^2
300	0.817 (7)	−0.8792 (8)	0.927 (4)
750	2.16 (18)	−0.9890 (10)	1.063 (5)
1000	2.6 (2)	−1.0410 (12)	1.142 (6)
1500	3.4 (3)	−1.1454 (14)	1.305 (7)
2000	4.0 (4)	−1.2528 (17)	1.477 (8)

Table 8. The Grüneisen parameter of $MgAl_2O_4$ spinel and their first and second derivatives with respect to pressure at various temperatures.

T K	γ_0	$\partial\gamma/\partial P$ 10^{-2}/GPa	$\partial^2\gamma/\partial P^2$ 10^{-4}/GPa^2
300	1.57 (13)	−1.391 (2)	0.832 (5)
750	1.15 (5)	−1.106 (2)	0.825 (5)
1000	1.12 (3)	−1.130 (2)	0.912 (6)
1500	1.117 (17)	−1.214 (2)	1.078 (7)
2000	1.136 (3)	−1.295 (2)	1.205 (8)

Generally, the effects of pressure on α and S values of $MgAl_2O_4$ spinel increase along with the increasing temperature (Tables 5 and 7). Whereas the pressure effects on C_P and γ decrease with the temperature at first, then start to increase or vary a little above a certain temperature, respectively (Tables 6 and 8). At room temperature conditions, the first pressure derivative of α is $(\partial\alpha/\partial P)_T = -5.385\ (7) \times 10^{-7}$/K·GPa, then the value decreases with the temperature to $-8.731\ (18) \times 10^{-7}$/K·GPa at 2000 K (Table 5). Additionally, the first pressure derivative of the entropy $(\partial S/\partial P)_T$ decreases from −0.8792 (8) J/mol·K·GPa to −1.2528 (17) J/mol·K·GPa in a temperature range of 300–2000 K (Table 7).

On the other hand, the first pressure derivatives of C_P and γ as functions of temperature are shown in Figure 7. The $(\partial C_P/\partial P)_T$ of $MgAl_2O_4$ spinel at room temperature conditions is determined as −0.0921 (3) J/mol·K·GPa (Table 6). The value increases with the temperature to −0.1055 (2) J/mol·K·GPa at ~400 K, then decreases to −0.4372 (11) J/mol·K·GPa at 2000 K (Table 6, Figure 7). For the Grüneisen parameter of $MgAl_2O_4$ spinel, the value of $(\partial\gamma/\partial P)_T$ is determined as $-1.391\ (2) \times 10^{-2}$/GPa at room temperature (Table 8). Similar to the heat capacity, the value of $(\partial\gamma/\partial P)_T$ tends to increase with the temperature to $-1.105\ (2) \times 10^{-2}$/GPa at ~700 K, then almost remains constant as $-1.295\ (2) \times 10^{-2}$/GPa to 2000 K (Table 8, Figure 7).

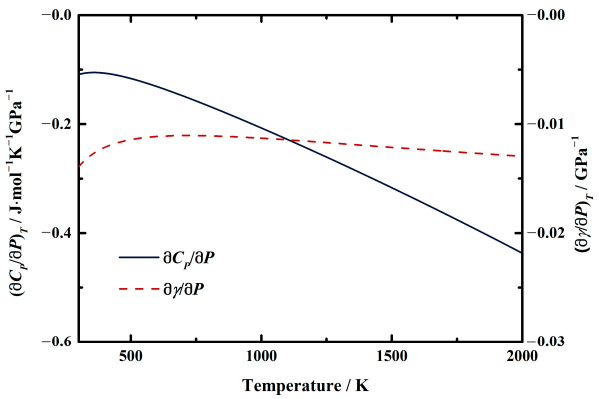

Figure 7. First pressure derivatives of heat capacity and Grüneisen parameter of $MgAl_2O_4$ spinel as a function of temperature.

4. Conclusions

In summary, following a numerical iterative procedure, we obtained self-consistent thermodynamic parameters: thermal expansion, heat capacity, entropy, and Grüneisen parameters of $MgAl_2O_4$ spinel in a wide *P-T* range. All these thermodynamic parameters are nonlinearly and negatively correlated with pressure. Besides, the pressure effects on the thermal expansion and entropy increase with temperature, while the first pressure derivatives of the heat capacity and Grüneisen parameter increase to a maximum at ~400 K and ~700 K, respectively, then decrease with temperature again. This paper just provides a basic understanding of the thermodynamic properties of $MgAl_2O_4$ spinel at HT-HPs. Further work needs to be carried out to obtain more accurate thermodynamic properties when considering the phase transitions of $MgAl_2O_4$ spinel.

Author Contributions: Conceptualization, C.S. and Y.L.; methodology, C.S. and Y.L.; formal analysis, W.Q.; investigation, W.Q.; resources, W.S.; writing—original draft preparation, C.S.; writing—review and editing, C.S. and W.Q.; supervision, Y.L.; project administration, Y.L. and C.S.; funding acquisition, Y.L., C.S. and W.Q. All authors have read and agreed to the published version of the manuscript.

Funding: This research was funded by the National Natural Science Foundation of China (Grant numbers: 41873075 and 42174225), the Key Research Program of Frontier Sciences of CAS (Grant number: ZDBS-LY-DQC015), the Natural Science Foundation of Hebei Province of China (Grant number: D2022512007), and project on scientific and technological innovation ability training of college and high school students of Hebei Province (Grant number: 22E50460D).

Data Availability Statement: Data is contained within the article.

Acknowledgments: We thank Wenge Zhou at the Institute of Geochemistry, Chinese Academy of Sciences for helpful discussions and suggestions. We are also grateful to Jinhan Yu, Xiang Ji, Xujie Guan, and Jinshuo Zhang at the School of Earth Sciences, Institute of Disaster Prevention.

Conflicts of Interest: The authors declare no conflict of interest.

References

1. Irifune, T.; Fujino, K.; Ohtani, E. A New High-pressure Form of $MgAl_2O_4$. *Nature* **1991**, *349*, 409–411. [CrossRef]
2. Klym, H.; Karbovnyk, I.; Piskunov, S.; Popov, A.I. Positron Annihilation Lifetime Spectroscopy Insight on Free Volume Conversion of Nanostructured $MgAl_2O_4$ Ceramics. *Nanomaterials* **2021**, *11*, 3373. [CrossRef] [PubMed]
3. Lushchik, A.; Feldbach, E.; Kotomin, E.A.; Kudryavtseva, I.; Kuzovkov, V.N.; Popov, A.I.; Seeman, V.; Shablonin, E. Distinctive Features of Diffusion-controlled Radiation Defect Recombination in Stoichiometric Magnesium Aluminate Spinel Single Crystals and Transparent Polycrystalline Ceramics. *Sci. Rep.* **2020**, *10*, 7810. [CrossRef]
4. Fumagalli, P.; Klemme, S. Mineralogy of the Earth: Phase Transitions and Mineralogy of the Upper Mantle. In *Treatise on Geophysics*; Schubert, G., Ed.; Elsevier: Oxford, UK, 2015; pp. 7–31. [CrossRef]
5. Chang, Z.P.; Barsch, G.R. Pressure Dependence of Single-crystal Elastic Constants and Anharmonic Properties of Spinel. *J. Geophys. Res.* **1973**, *78*, 2418–2433. [CrossRef]
6. Yoneda, A. Pressure Derivatives of Eastic Constants of Single Crystal MgO and $MgAl_2O_4$. *J. Phys. Earth* **1990**, *38*, 19–55. [CrossRef]
7. Cynn, H.; Anderson, O.L.; Nicol, M. Effects of Cation Disordering in a Natural $MgAl_2O_4$ Spinel Observed by Rectangular Parallelepiped Ultrasonic Resonance and Raman Measurements. *Pure Appl. Geophys.* **1993**, *141*, 415–444. [CrossRef]
8. Askarpour, V.; Manghnani, M.H.; Fassbender, S.; Yoneda, A. Elasticity of Single-crystal $MgAl_2O_4$ Spinel up to 1273 K by Brillouin Spectroscopy. *Phys. Chem. Miner.* **1993**, *19*, 511–519. [CrossRef]
9. Chopelas, A. The Fluorescence Sideband Method for Obtaining Acoustic Velocities at High Compressions: Application to MgO and $MgAl_2O_4$. *Phys. Chem. Miner.* **1996**, *23*, 25–37. [CrossRef]
10. Kruger, M.B.; Nguyen, J.H.; Caldwell, W.; Jeanloz, R. Equation of State of $MgAl_2O_4$ Spinel to 65 GPa. *Phys. Rev. B* **1997**, *56*, 1–4. [CrossRef]
11. Suzuki, I.; Ohno, I.; Anderson, O.L. Harmonic and Anharmonic Properties of Spinel $MgAl_2O_4$. *Am. Mineral.* **2000**, *85*, 304–311. [CrossRef]
12. Levy, D.; Pavese, A.; Hanfland, M. Synthetic $MgAl_2O_4$ (spinel) at High-pressure Conditions (0.0001–30 GPa): A synchrotron X-ray Powder Diffraction Study. *Am. Mineral.* **2003**, *88*, 93–98. [CrossRef]
13. Nestola, F.; Ballaran, T.B.; Balic-Zunic, T.; Princivalle, F.; Secco, L.; Dal Negro, A. Comparative Compressibility and Structural Behavior of Spinel $MgAl_2O_4$ at High Pressures: The Independency on the Degree of Cation Order. *Am. Mineral.* **2007**, *92*, 1838–1843. [CrossRef]

14. Zou, Y.; Gréaux, S.; Irifune, T.; Li, B.; Higo, Y. Unusual Pressure Effect on the Shear Modulus in $MgAl_2O_4$ Spinel. *J. Phys. Chem. C* **2013**, *117*, 24518–24526. [CrossRef]
15. Duan, Y.; Li, X.; Sun, N.; Ni, H.; Tkachev, S.N.; Mao, Z. Single-crystal Elasticity of $MgAl_2O_4$-spinel up to 10.9 GPa and 1000 K: Implication for the Velocity Structure of the Top Upper Mantle. *Earth Planet. Sci. Lett.* **2018**, *481*, 41–47. [CrossRef]
16. Hagiwara, Y.; Angel, R.J.; Yamamoto, J.; Alvaro, M. Equation of State of Spinel ($MgAl_2O_4$): Constraints on Self-consistent Thermodynamic Parameters and Implications for Elastic Geobarometry of Peridotites and Chromitites. *Contrib. Mineral. Petrol.* **2022**, *177*, 108. [CrossRef]
17. Suzuki, I.; Kumazawa, M. Anomalous Thermal Expansion in Spinel $MgAl_2O_4$. *Phys. Chem. Miner.* **1980**, *5*, 279–284. [CrossRef]
18. Samui, P.; Gupta, N.K.; Dash, S.; Dahale, N.D.; Naik, Y. Thermoluminescence and Linear Thermal Expansion of $MgAl_2O_4$. *J. Therm. Anal. Calorim.* **2013**, *115*, 1289–1294. [CrossRef]
19. Singh, H.P.; Simmons, G.; McFarlin, P.F. Thermal Expansion of Natural Spinel, Ferroan Gahnite, Magnesiochromite and Synthetic Spinel. *Acta Crystallogr. Sect. A* **1975**, *31*, 820–822. [CrossRef]
20. Yamanaka, T.; Takéuchi, Y. Order-disorder Transition in $MgAl_2O_4$ Spinel at High Temperatures up to 1700 °C. *Z. Krist.—Cryst. Mater.* **1983**, *165*, 65–78. [CrossRef]
21. Grimes, N.W.; Al-Ajaj, E.A. Low-temperature Thermal Expansion of Spinel. *J. Phys. Condens. Matter* **1992**, *4*, 6375–6380. [CrossRef]
22. Fiquet, G.; Richet, P.; Montagnac, G. High-temperature Thermal Expansion of Lime, Periclase, Corundum and Spinel. *Phys. Chem. Miner.* **1999**, *27*, 103–111. [CrossRef]
23. Carbonin, S.; Martignago, F.; Menegazzo, G.; Dal Negro, A. X-ray Single-Crystal Study of Spinels: In situ Heating. *Phys. Chem. Miner.* **2002**, *29*, 503–514. [CrossRef]
24. Peterson, R.C.; Lager, G.A.; Hitterman, R.L. A Time-of-flight Neutron Powder Diffraction Study of $MgAl_2O_4$ at Temperatures up to 1273 K. *Am. Mineral.* **1991**, *76*, 1455–1458.
25. Redfern, S.A.T.; Harrison, R.J.; O'Neill, H.S.C.; Wood, D.R.R. Thermodynamics and Kinetics of Cation Ordering in $MgAl_2O_4$ Spinel up to 1600°C from in situ Neutron Diffraction. *Am. Mineral.* **1999**, *84*, 299–310. [CrossRef]
26. Pavese, A.; Artioli, G.; Hoser, A. $MgAl_2O_4$ Synthetic Spinel: Cation and Vacancy Distribution as a Function of Temperature, from in situ Neutron Powder Diffraction. *Z. Krist.—Cryst. Mater.* **2000**, *215*, 406–412. [CrossRef]
27. Birch, F. Finite Strain Isotherm and Velocities for Single-crystal and Polycrystalline NaCl at High Pressures and 300 K. *J. Geophys. Res.* **1978**, *83*, 1257–1268. [CrossRef]
28. Jackson, I.; Rigden, S.M. Analysis of P-V-T data: Constraints on the thermoelastic properties of high-pressure minerals. *Phys. Earth Planet. Inter.* **1996**, *96*, 85–112. [CrossRef]
29. King, E.G. Heat Capacities at Low Temperatures and Entropies at 298.16 K. of Crystalline Calcium and Magnesium Aluminates. *J. Phys. Chem.* **1955**, *59*, 218–219. [CrossRef]
30. Bonnickson, K.R. High Temperature Heat Contents of Aluminates of Calcium and Magnesium. *J. Phys. Chem.* **1955**, *59*, 220–221. [CrossRef]
31. Richet, P.; Fiquet, G. High-temperature Heat Capacity and Premelting of Minerals in the System MgO-CaO-Al_2O_3-SiO_2. *J. Geophys. Res.* **1991**, *96*, 445–456. [CrossRef]
32. Klemme, S.; Ahrens, M. Low-temperature Heat Capacities of $MgAl_2O_4$ and Spinels of the $MgCr_2O_4$–$MgAl_2O_4$ Solid Solution. *Phys. Chem. Miner.* **2007**, *34*, 59–72. [CrossRef]
33. Mao, X.-C.; Liu, K.; Hou, B.-S.; Tan, J.; Zhou, X.-L. Theoretical Investigation of the Structural, Elastic, and Thermodynamic Properties of MgAl2O4 Spinel under High Pressure. *J. Phys. Soc. Jpn.* **2016**, *85*, 114605. [CrossRef]
34. Holland, T.J.B.; Powell, R. An Improved and Extended Internally Consistent Thermodynamic Dataset for Phases of Petrological Interest, Involving a New Equation of State for Solids. *J. Metamorph. Geol.* **2011**, *29*, 333–383. [CrossRef]
35. Faccincani, L.; Faccini, B.; Casetta, F.; Mazzucchelli, M.; Nestola, F.; Coltorti, M. EoS of Mantle Minerals Coupled with Composition and Thermal State of the Lithosphere: Inferring the Density Structure of Peridotitic Systems. *Lithos* **2021**, *404*, 106483. [CrossRef]
36. Davis, L.A.; Gordon, R.B. Compression of Mercury at High Pressure. *J. Chem. Phys.* **1967**, *46*, 2650–2660. [CrossRef]
37. Ayrinhac, S.; Gauthier, M.; Bove, L.E.; Morand, M.; Le Marchand, G.; Bergame, F.; Philippe, J.; Decremps, F. Equation of State of Liquid Mercury to 520 K and 7 GPa from Acoustic Velocity Measurements. *J. Chem. Phys.* **2014**, *140*, 244201. [CrossRef]
38. Ayrinhac, S.; Gauthier, M.; Le Marchand, G.; Morand, M.; Bergame, F.; Decremps, F. Thermodynamic Properties of Liquid Gallium from Picosecond Acoustic Velocity Measurements. *J. Phys.-Condes. Matter* **2015**, *27*, 275103. [CrossRef]
39. Su, C.; Fan, D.; Jiang, J.; Sun, Z.; Liu, Y.; Song, W.; Wan, Y.; Yang, G.; Qiu, W. Self-Consistent Thermodynamic Parameters of Diopside at High Temperatures and High Pressures: Implications for the Adiabatic Geotherm of an Eclogitic Upper Mantle. *Minerals* **2021**, *11*, 1322. [CrossRef]
40. Su, C.; Liu, Y.; Fan, D.; Song, W.; Yang, G. Self-consistent Thermodynamic Parameters of Pyrope and Almandine at High-temperature and High-pressure Conditions: Implication on the Adiabatic Temperature Gradient. *Phys. Earth Planet. Inter.* **2022**, *322*, 106789. [CrossRef]
41. Su, C.; Liu, Y.; Fan, D.; Song, W.; Jiang, J.; Sun, Z.; Yang, G. Thermodynamic Properties of Fe-Bearing Wadsleyite and Determination of the Olivine-Wadsleyite Phase Transition Boundary in $(Mg,Fe)_2SiO_4$ System. *Front. Earth Sci.* **2022**, *10*, 879678. [CrossRef]
42. Johari, G.P. Entropy, Enthalpy and Volume of Perfect Crystals at Limiting High Pressure and the Third Law of Thermodynamics. *Thermochim. Acta* **2021**, *698*, 178891. [CrossRef]

43. Andreozzi, G.B.; Princivalle, F. Kinetics of Cation Ordering in Synthetic $MgAl_2O_4$ Spinel. *Am. Mineral.* **2002**, *87*, 838–844. [CrossRef]
44. Shukla, P.; Chernatynskiy, A.; Nino, J.C.; Sinnott, S.B.; Phillpot, S.R. Effect of Inversion on Thermoelastic and Thermal Transport Properties of $MgAl_2O_4$ Spinel by Atomistic Simulation. *J. Mater. Sci.* **2010**, *46*, 55–62. [CrossRef]
45. Ma, Y.; Bao, X.; Liu, X. Thermodynamics of Mg–Al Order-Disorder Reaction in $MgAl_2O_4$-Spinel: Constrained by Prolonged Annealing Experiments at 773–1123 K. *Molecules* **2021**, *26*, 872. [CrossRef] [PubMed]
46. Gonzalez-Platas, J.; Alvaro, M.; Nestola, F.; Angel, R. EosFit7-GUI: A New Graphical User Interface for Equation of State Calculations, Analyses and Teaching. *J. Appl. Crystallogr.* **2016**, *49*, 1377–1382. [CrossRef]
47. Fei, Y. Thermal Expansion. In *Mineral Physics & Crystallography*; Ahrens, T.J., Ed.; AGU Reference Shelf; AGU Publications: Washington, DC, USA, 1995; pp. 29–44. [CrossRef]
48. Haas, J.L.; Fisher, J.R. Simultaneous Evaluation and Correlation of Thermodynamic Data. *Am. J. Sci.* **1976**, *276*, 525–545. [CrossRef]
49. Berman, R.G.; Brown, T.H. Heat Capacity of Minerals in the System Na_2O-K_2O-CaO-MgO-FeO-Fe_2O_3-Al_2O_3-SiO_2-TiO_2-H_2O-CO_2: Representation, Estimation, and High Temperature Extrapolation. *Contrib. Mineral. Petrol.* **1985**, *89*, 168–183. [CrossRef]
50. Speziale, S.; Nestola, F.; Jiang, F.; Duffy, T.S. Single-crystal Elastic Constants of Spinel ($MgAl_2O_4$) to 11.1 GPa by Brillouin Scattering. In Proceedings of the AGU Fall Meeting, San Francisco, CA, USA, 12–16 December 2016; p. MR23A-2658.
51. Bruschini, E.; Speziale, S.; Bosi, F.; Andreozzi, G.B. Fe–Mg Substitution in Aluminate Spinels: Effects on Elastic Properties Investigated by Brillouin Scattering. *Phys. Chem. Miner.* **2018**, *45*, 759–772. [CrossRef]
52. Núñez-Valdez, M.; Bruschini, E.; Speziale, S.; Bosi, F.; Fregola, R.A.; D'Ippolito, V.; Andreozzi, G.B. Reexploring the Cation Ordering and Magnetic Cation Substitution Effects on the Elastic Anisotropy of Aluminum Spinels. *J. Appl. Phys.* **2018**, *124*, 175901. [CrossRef]
53. Berman, R.G. Internally-Consistent Thermodynamic Data for Minerals in the System Na_2O-K_2O-CaO-MgO-FeO-Fe_2O_3-Al_2O_3-SiO_2-TiO_2-H_2O-CO_2. *J. Petrol.* **1988**, *29*, 445–522. [CrossRef]
54. Robie, R.A.; Hemingway, B.S. *Thermodynamic Properties of Minerals and Related Substances at 298.15 K and 1 bar (105 Pascals) Pressure and at Higher Temperature*; U.S. Geological Survey, Information Services: Reston, VA, USA, 1995; p. 461. [CrossRef]
55. Vočadlo, N.L.; Price, G.D. The Grüneisen Parameter-Computer Calculations via Lattice Dynamics. *Phys. Earth Planet. Inter.* **1994**, *82*, 261–270. [CrossRef]